CHALMERS
FINITE ELEMENT CENTER

PREPRINT 2003–02

Application of the Local Nonobtuse Tetrahedral Refinement Techniques Near Fichera-like Corners

Larisa Beilina, Sergey Korotov, Michal Křížek

Chalmers Finite Element Center
CHALMERS UNIVERSITY OF TECHNOLOGY
Göteborg Sweden 2003

CHALMERS FINITE ELEMENT CENTER

Preprint 2003–02

Application of the Local Nonobtuse Tetrahedral Refinement Techniques Near Fichera-like Corners

Larisa Beilina, Sergey Korotov, Michal Křížek

Chalmers Finite Element Center
Chalmers University of Technology
SE–412 96 Göteborg Sweden
Göteborg, February 2003

Application of the Local Nonobtuse Tetrahedral Refinement Techniques Near Fichera-like Corners
Larisa Beilina, Sergey Korotov, Michal Křížek
NO 2003–02
ISSN 1404–4382

Chalmers Finite Element Center
Chalmers University of Technology
SE–412 96 Göteborg
Sweden
Telephone: +46 (0)31 772 1000
Fax: +46 (0)31 772 3595
www.phi.chalmers.se

Printed in Sweden
Chalmers University of Technology
Göteborg, Sweden 2003

APPLICATION OF THE LOCAL NONOBTUSE TETRAHEDRAL REFINEMENT TECHNIQUES NEAR FICHERA-LIKE CORNERS

LARISA BEILINA, SERGEY KOROTOV, AND MICHAL KŘÍŽEK

ABSTRACT. Linear tetrahedral finite elements whose all dihedral angles are nonobtuse guarantee the validity of the discrete maximum principle for a wide class of second order elliptic and parabolic problems. In this paper we present an algorithm which generates nonobtuse face-to-face tetrahedral partitions that refine locally in a neighborhood of a given vertex of a polyhedral domain. Three numerical examples show how to treat singularities of solutions and their derivatives at Fichera-like corners using the proposed local nonobtuse tetrahedral refinements for the Poisson equation with Dirichlet boundary conditions.

Keywords: partial differential equations, finite element method, nonobtuse tetrahedra, linear tetrahedral finite elements, discrete maximum principle, reentrant corner, nonlinear heat conduction

Mathematics Subject Classification (1991): 65N30, 65N50, 51M20

Date: 5th February 2003.

Larisa Beilina, Department of Mathematics, Chalmers University of Technology, S–412 96 Göteborg, Sweden, *email*: larisa@math.chalmers.se

Sergey Korotov, Department of Mathematical Information Technology University of Jyväskylä P.OḂox 35, FIN–400 14 Jyväskylä, Finland *email*: korotovmit.jyu.fi

Michal Křížek Mathematical Institute, Academy of Sciences, Žitná 25, CZ–115 67 Prague 1, Czech Republic *e-mail*: krizekmath.cas.cz.

1. Introduction

Linear tetrahedral finite elements are commonly used for solving second order boundary value problems. The structure and properties of the associated stiffness matrices essentially depend on the dihedral angles between faces of tetrahedral elements. To see this fact, let us consider an arbitrary tetrahedron $ABCD$. Let p and q be two linear affine functions such that

$$\begin{aligned} p(A) = 1, \quad p(B) = p(C) = p(D) = 0, \\ q(B) = 1, \quad q(A) = q(C) = q(D) = 0, \end{aligned}$$

then a straightforward calculation leads to the following formula (see [13, p. 63] for the proof)

$$\nabla p \cdot \nabla q = -\frac{\text{meas}_2 ACD \ \text{meas}_2 BCD}{9\,(\text{meas}_3 ABCD)^2} \cos\alpha, \tag{1.1}$$

where α is the angle between the faces ACD and BCD (see Figure 1) and the symbol meas_d stands for d-dimensional measure. If $\alpha > \pi/2$, then the scalar product in (1.1) is obviously positive. Hence, each obtuse dihedral angle of the tetrahedron $ABCD$ gives a positive contribution to the corresponding off-diagonal entry of the element (and also global) stiffness matrix, when solving a boundary value problem with the Laplace operator.

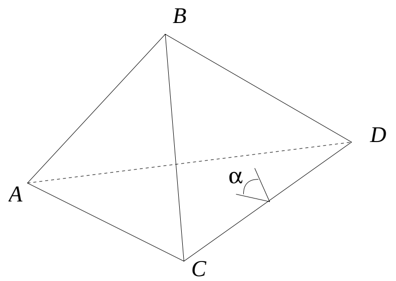

Figure 1. A general tetrahedron whose two faces include the angle α.

Note that the same is also true for a wider class of nonlinear elliptic problems of the form (see [14])

$$-\nabla \cdot (\lambda(x, u, \nabla u)\nabla u) = f(x) \quad \text{in} \quad \Omega, \tag{1.2}$$

$$u = 0 \quad \text{on} \quad \partial\Omega, \tag{1.3}$$

where λ is a positive smooth function and Ω is a bounded polyhedral domain with a Lipschitz-continuous boundary $\partial\Omega$. Equations (1.2)–(1.3) describe, for instance, a stationary nonlinear heat conduction.

Recall that a tetrahedron is said to be *nonobtuse* if all six dihedral angles between its faces are less than or equal $\pi/2$. In this paper, we shall use only face-to-face tetrahedral partitions of $\overline{\Omega}$, which are called, for simplicity, *partitions*. A partition is said to be *nonobtuse* if it only contains nonobtuse tetrahedra.

According to [14], linear elements applied to problem (1.2)–(1.3) on nonobtuse partitions yield irreducibly diagonally dominant stiffness matrices (whose all off-diagonal entries are nonpositive). It is well known (see [5, Chapt. II.4.3] or [17, p. 85]) that such matrices are monotone. This enables us to prove easily the L^∞-convergence of the finite element method like in [9], where a two-dimensional nonlinear problem is solved on nonobtuse triangulations. Nonobtuse tetrahedral partitions also guarantee the validity of the discrete maximum principle for the problem (1.2)–(1.3), i.e., we have $u_h \leq 0$ provided $f \leq 0$, where u_h is the Galerkin approximation of the solution of (1.2)–(1.3). In other words, u_h attains its maximum on the boundary $\partial\Omega$, if the homogeneous Dirichlet boundary conditions and nonpositive right-hand sides are considered. For the results on the validity of the discrete maximum principle for parabolic problems on nonobtuse simplicial meshes, we refer to [10].

In [11], we give a global refinement procedure yielding nonobtuse tetrahedra over the whole domain. However, such a technique requires a large amount of computer time and also computer memory to store the associated stiffness matrix. Therefore, in the present paper we introduce a local refinement procedure yielding nonobtuse partitions that refine only near a particular vertex, where a singularity of the exact solution may appear (see [8], [16]).

In Section 2, we show that the discrete maximum principle can be violated for standard trilinear block finite elements. In Section 3, we define a special tetrahedron — a path tetrahedron — and show how to generate nonobtuse partitions that refine near one of its vertices. In Section 4, we generalize this refinement procedure to a neighborhood of the Fichera-like corners. Section 5 is devoted to several numerical tests.

2. Breakdown of the discrete maximum principle for trilinear block elements

According to [13], some dihedral angles of linear tetrahedral elements can be slightly larger than $\pi/2$ and the discrete maximum principle for the Poisson equation with the Dirichlet boundary conditions is still valid. On the other hand, the popular trilinear block elements do not preserve the discrete maximum principle, in general. To see this fact let $\Omega = (0,6)\times(0,3)\times(0,3)$ be decomposed into $3\times3\times3$ congruent blocks whose edges have lengths $a = 2$ and $b = c = 1$. Consequently, there are 8 interior nodes. Let us assume that they are ordered lexicographically. Using the trilinear finite elements for problem (1.2)–(1.3) with $\lambda \equiv 1$, we find that certain off-diagonal entries of the associated stiffness matrix $\mathbf{A} = (A_{ij})_{i,j=1}^{8}$ are positive, for instance (see [15, p. 68] for details),

$$A_{12} = 4\Big(\frac{ab}{18c} + \frac{ac}{18b} - \frac{bc}{9a}\Big) = \frac{2}{3}.$$

Similarly, we can find that

$$A_{11} = 8\Big(\frac{ab}{9c} + \frac{ac}{9b} + \frac{bc}{9a}\Big) = 4, \quad A_{18} = -\frac{ab}{36c} - \frac{ac}{36b} - \frac{bc}{36a} = -\frac{1}{8},$$

etc., and thus the whole stiffness matrix reads

$$\mathbf{A} = \frac{1}{24}\begin{pmatrix} 96 & & & & & & & \\ 16 & 96 & & & & & \text{sym.} & \\ -8 & -4 & 96 & & & & & \\ -4 & -8 & 16 & 96 & & & & \\ -8 & -4 & -10 & -3 & 96 & & & \\ -4 & -8 & -3 & -10 & 16 & 96 & & \\ -10 & -3 & -8 & -4 & -8 & -4 & 96 & \\ -3 & -10 & -4 & -8 & -4 & -8 & 16 & 96 \end{pmatrix}.$$

It is easy to calculate that $\mathbf{A}$ is not monotone, since some entries of the inverse matrix $\mathbf{A}^{-1} = (A_{ij}^{-1})_{i,j=1}^{8}$ are negative, e.g., $A_{12}^{-1} \doteq -0.039766$. Hence, globally nonpositive heat sources f, corresponding to the discrete right-hand side $\mathbf{f} = (0, -1, 0, 0, 0, 0, 0, 0)^{\top}$, yield paradoxically a positive temperature $u_1 = (\mathbf{A}^{-1}\mathbf{f})_1 = -A_{12}^{-1} \doteq 0.039766$ at the first node. This means that the numerical heat flows from colder to warmer parts of the computational domain, which destroys the reliability of numerical solution. That is why it is important to keep the validity of the maximum principle in the discrete case.

3. Local nonobtuse refinements of a path tetrahedron

Definition 3.1. A tetrahedron is said to be a *path tetrahedron* if it has three mutually perpendicular edges which do not pass through the same vertex.

The reason for the name of the above tetrahedron is that its three perpendicular edges form a "path" (see [4]).

Proposition 3.2. *Any path tetrahedron is nonobtuse.*

For the proof see [11, p. 728–729].

A typical example of a path tetrahedron is illustrated in Figure 2 (all its right angles, solid and dihedral, are indicated there).

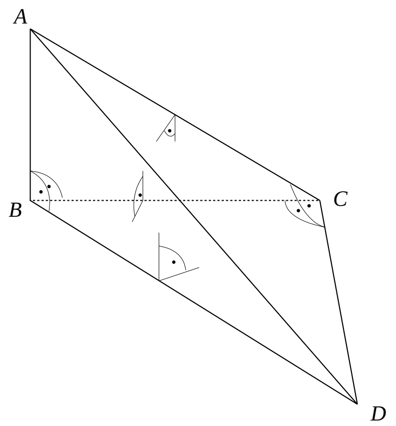

Figure 2. A path tetrahedron.

The main idea of generating local nonobtuse tetrahedral refinements is exposed in the following theorem, whose proof is constructive.

Theorem 3.3. *Let $ABCD$ be a path tetrahedron whose edges AB, BC, and CD are mutually perpendicular. Then there exists an infinite family of nonobtuse partitions of this tetrahedron into path tetrahedra that locally refine in a neighborhood of the vertex A.*

P r o o f . Let P be the orthogonal projection of the point B onto the line AC. Obviously, P lies in the interior of the line segment AC, since ABC is the right triangle.

Further, let Q be the orthogonal projection of the point P onto the line AD. Since ACD is a right triangle, APD has an obtuse angle at P, and thus the point Q lies in the interior of the line segment AD.

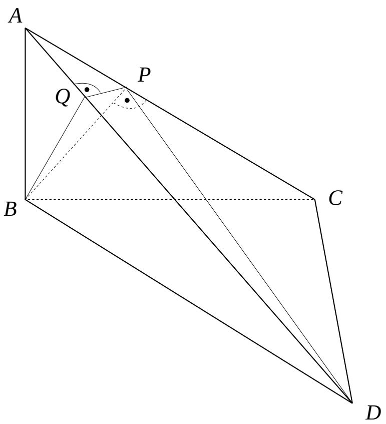

Figure 3. Partition of a path tetrahedron $ABCD$ into three path tetrahedra.

We observe that the line segment BP is perpendicular to the face ACD. Therefore, BP is perpendicular to any line which is contained in the plane ACD. From this property we easily find that the original tetrahedron $ABCD$ can be decomposed into the following three path tetrahedra (see Figure 3):

$$\begin{array}{lll} BPCD & \text{with} & BP \perp PC \perp CD \perp BP, \\ BPQD & \text{with} & BP \perp PQ \perp QD \perp BP, \\ AQPB & \text{with} & AQ \perp QP \perp PB \perp AQ. \end{array}$$

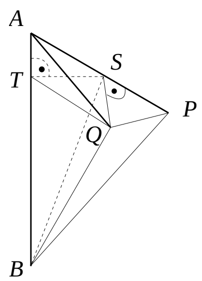

Figure 4. Partition of a path tetrahedron $ABQP$ into three path tetrahedra.

Now we decompose the last path subtetrahedron $AQPB$ again into three path subtetrahedra following the same rules as above. Let S be the orthogonal projection of the point Q onto the line AP, and let T be the orthogonal projection of the point S onto the line AB. Then the path tetrahedron $AQPB$ can be decomposed into the following three path subtetrahedra (see Figure 4):

$$\begin{array}{lll} QSPB & \text{with} & QS \perp SP \perp PB \perp QS, \\ QSTB & \text{with} & QS \perp ST \perp TB \perp QS, \\ ATSQ & \text{with} & AT \perp TS \perp SQ \perp AT. \end{array}$$

Consequently, the five path subtetrahedra $BPCD$, $BPQD$, $QSPB$, $QSTB$, and $ATSQ$ form a face-to-face partition of the original path tetrahedron $ABCD$ (see Figure 5).

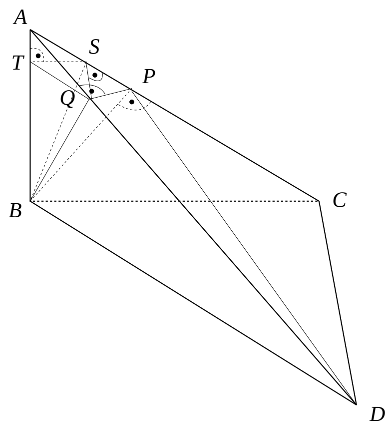

Figure 5. Final partition of a path tetrahedron $ABCD$ into five path tetrahedra.

Since S is the orthogonal projection of Q onto the line AC, the line segments QS and DC are parallel. Similarly we find that TS and BC are parallel, since T is the orthogonal projection of S onto the line AB. From here we conclude that the face TSQ is parallel to BCD, and thus, the path subtetrahedron $ATSQ$ is similar to the original tetrahedron $ABCD$.

The subtetrahedron $ATSQ$ can be now decomposed into 5 subtetrahedra in a similar way as $ABCD$, and thus we can get further refinement near the vertex A. By this reccurence procedure, we obtain the required infinite family of nonobtuse face-to-face tetrahedral partitions. $\square$

4. Local nonobtuse refinements near Fichera-like corners

In [12], we proposed an algorithm for a local nonobtuse tetrahedral refinement of a cube in the neigbourhood of one of its vertices. If several cubes meet at one point, then we can apply this algorithm to each of them so that the whole partition remains face-to-face. For instance, in Figure 6 we see local nonobtuse tetrahedral refinements of a polyhedral domain $\Omega = (-1,1)^3 \setminus [0,1)^3$, which presents the union of 7 cubes. The concave (reentrant) corner of such a domain is called the *Fichera corner* or sometimes the *Fichera vertex* (see, e.g., [1, 2, 3, 16]).

Actually, the algorithm from [12] can also be viewed as the following procedure: we divide first a cube into six path tetrahedra (cf. Figure 7b), and further make a local nonobtuse tetrahedral refinement of each of the path tetrahedra toward to one of their two common vertices so that the overall partition of the cube remains always conforming.

If the algorithm from [12] is percieved as above, we immediately observe that the corresponding local refinement of a single path tetrahedron coincides with the refinement procedure presented in Section 3, applied to a particular type of path tetrahedra – when the three mutually perpendicular edges are of the same length.

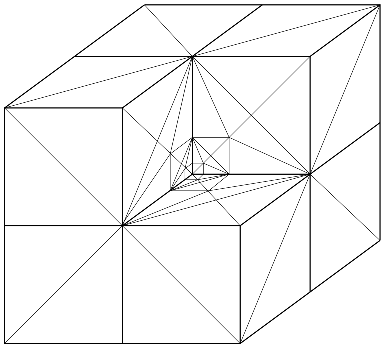

Figure 6. Local nonobtuse refinement of the Fichera domain.

The above comparison of two refinement procedures immediately suggests the next generalization step, leading to a refinement procedure for more general corners of a polyhedral domain, which we will refer to as Fichera-like corners. In particular, now we introduce sufficient conditions which enable us to generate local refinements, involving nonobtuse partitions near a given vertex:

(i) Let $T_1, \ldots, T_k$ be tetrahedra from an initial partition, which share a given vertex A belonging to the longest edge of each T_i,

(ii) T_1 is a path tetrahedron,

(iii) each T_i is a mirror image of any adjacent tetrahedron T_j with respect to their common triangular face $T_i \cap T_j$, $i, j \in \{1, \ldots, k\}$.

In Figure 7, we observe three examples of clusters of path tetrahedra satisfying the above conditions (i)–(iii). Note that in Figure 7a, the "lower" face is an equilateral triangle, in Figure 7b, we have a cube, and in Figure 7c, the "rectangular" face is a square.

Now, let us consider a family of nonobtuse partitions of T_1 whose existence is guaranteed by Theorem 3.3. All adjacent tetrahedra to T_1 that share the vertex A are mirror images of T_1. Therefore, their refinements will be defined as mirror images of refinements of T_1. Similarly, we define refinements of all the other tetrahedra. Obviously, this construction preserves the overall face-to-face property of partitions.

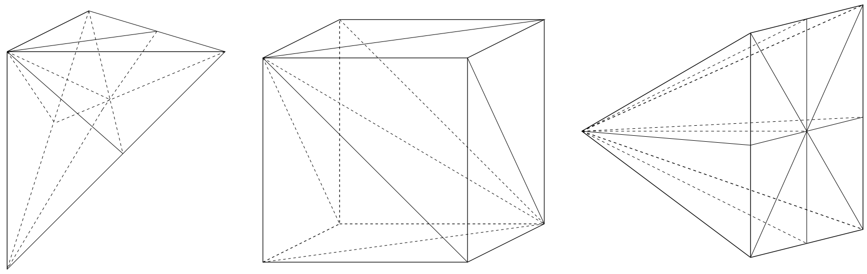

Figure 7. Clusters of path tetrahedra.

5. Numerical tests in domains with Fichera-like corners

In this section, we compare the performance of the local mesh refinement procedure on computer implementation of the solution of the Poisson equation with the nonhomogeneous boundary condition

$$\begin{aligned} -\Delta u &= f \quad \text{in} \quad \Omega, \\ u &= \overline{u} \quad \text{on} \quad \partial\Omega, \end{aligned}$$

where $\overline{u} \in H^1(\Omega)$ is a given function.

The errors in Tables 1, 3, and 5 are L^2-norms of the difference between the exact solution u and the computed finite element solution u_h over domain Ω

$$\|u - u_h\|_0 = \Big(\int_\Omega |u - u_h|^2\, dx\Big)^{1/2}.$$

The errors in Tables 2, 4, and 6 are H^1-seminorms of the difference between gradients of u and u_h

$$|u - u_h|_1 = \Big(\int_\Omega |\nabla u - \nabla u_h|^2\, dx\Big)^{1/2}.$$

These errors do not form monotone sequences, in general, due to more precise numerical integration near the singularity after more refinement steps.

In order to calculate the entries of the stiffness matrix and the load vector, we employ the higher order numerical quadrature formulae on tetrahedra from [5, 6], with 4, 11, and 24 integration points, which are exact for all polynomials of the second, fourth, and sixth orders, respectively.

Example 5.1. Let $\Omega = ((-1,1)^2 \times (0,1)) \setminus ([0,1) \times (-1,0] \times (0,1))$, i.e., $\overline{\Omega}$ is the union of three unit cubes (see Figure 8). We shall take the right-hand side f so that the true solution u in the cylindrical coordinates (r, φ, z) reads

$$\tilde{u}(r, \varphi, z) = z^{1/2} r^{2/3} \sin(\tfrac{2}{3}\varphi).$$

and u satisfies the Poisson equation

$$-\Delta u = \frac{1}{4} z^{-3/2} r^{2/3} \sin(\tfrac{2}{3}\varphi).$$

nodes	elements	4 pts	11 pts	24 pts
16	18	0.0135088	0.0141321	0.0141394
38	87	0.0123574	0.0131168	0.0130618
60	159	0.0123575	0.0131169	0.0130619
82	231	0.0123575	0.0131169	0.0130619

Table 1: L^2-norm of the error for Example 5.1

nodes	elements	4 pts	11 pts	24 pts
16	18	0.182881	0.453355	1.27426
38	87	0.317062	0.562961	1.30833
60	159	0.327977	0.576841	1.32415
82	231	0.330272	0.580989	1.33239

Table 2: H^1-seminorm of the error for Example 5.1

Furthermore, we shall consider solutions of the form

$$u(x) = \left(\sqrt{x_1^2 + x_2^2 + x_3^2}\right)^q, \tag{5.1}$$

where $x = (x_1, x_2, x_3)$ and q is a real number, in the unit sphere. Using the standard spherical coordinates (r, φ, θ) and the substitution theorem, we get for $q > -\frac{1}{2}$ that

$$\begin{aligned}\|u\|_1^2 &= \int_0^1 \int_0^{2\pi} \int_0^{\pi} (r^{2q} + q^2 r^{2q-2}) r^2 \sin\theta \, d\theta \, d\varphi \, dr \\ &= 4\pi \int_0^1 (r^{2q+2} + q^2 r^{2q}) dr = 4\pi \Big(\frac{1}{2q+3} + \frac{q^2}{2q+1} \Big) \in (0, \infty),\end{aligned}$$

and the triple integral is not finite whenever $q \le -\frac{1}{2}$. The same will be true if we replace the unit sphere by the union of several cubes which contain the origin $(0, 0, 0)$.

The right-hand side $f = -\Delta u$ corresponding to the solution (5.1) is

$$f(x) = -q(q+1) \frac{u(x)}{x_1^2 + x_2^2 + x_3^2}.$$

Example 5.2. Let $\Omega = ((-1,1)^2 \times (-1,0)) \cup ((0,1)^2 \times [0,1))$, i.e., $\overline{\Omega}$ is the union of five unit cubes (see Figure 10). We set $q = \frac{1}{2}$ and take $\overline{u} = u$ on $\partial\Omega$, where u is given by (5.1).

nodes	elements	4 pts	11 pts	24 pts
22	30	0.0533061	0.0577743	0.0579317
84	265	0.0153702	0.0162520	0.0162535
115	385	0.0153585	0.0162387	0.0162401
146	505	0.0153585	0.0162387	0.0162401

Table 3: L^2-norm of the error for Example 5.2.

nodes	elements	4 pts	11 pts	24 pts
22	30	0.958325	1.028670	1.038700
84	265	0.590882	0.590969	0.590941
115	385	0.610457	0.610116	0.610112
146	505	0.713116	0.712898	0.712911

Table 4: H^1-seminorm of the error for Example 5.2.

Example 5.3. Let $\Omega = (-1,1)^3 \setminus [0,1)^3$, i.e., $\overline{\Omega}$ is the union of seven unit cubes (see Figure 12) and the Fichera corner is in the origin (0,0,0). We set $q = -\frac{1}{4}$, and again take $\overline{u} = u$ on $\partial\Omega$. In this case, the solution itself has a singularity at the origin, see (5.1).

nodes	elements	4 pts	11 pts	24 pts
26	42	0.3705270	0.3708450	0.3697510
100	371	0.0196610	0.0210155	0.0209284
137	539	0.0115099	0.0141417	0.0141224
174	707	0.0107786	0.0135825	0.0135698

Table 5: L^2-norm of the error for Example 5.3

nodes	elements	4 pts	11 pts	24 pts
26	42	1.97317	2.37207	2.54099
100	371	1.43409	1.45116	1.44991
137	539	2.79540	2.80079	2.80042
174	707	6.35086	6.35945	6.35787

Table 6: H^1-seminorm of the error for Example 5.3.

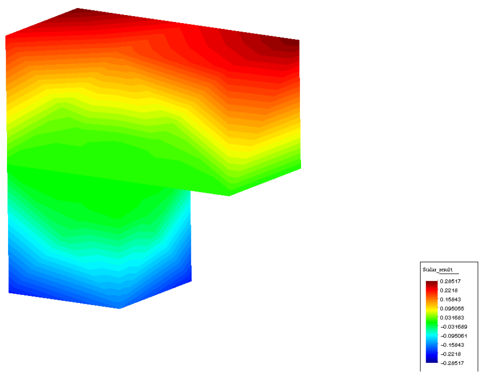

Figure 9. Computed solution on the three times refined mesh for Examples 5.1.

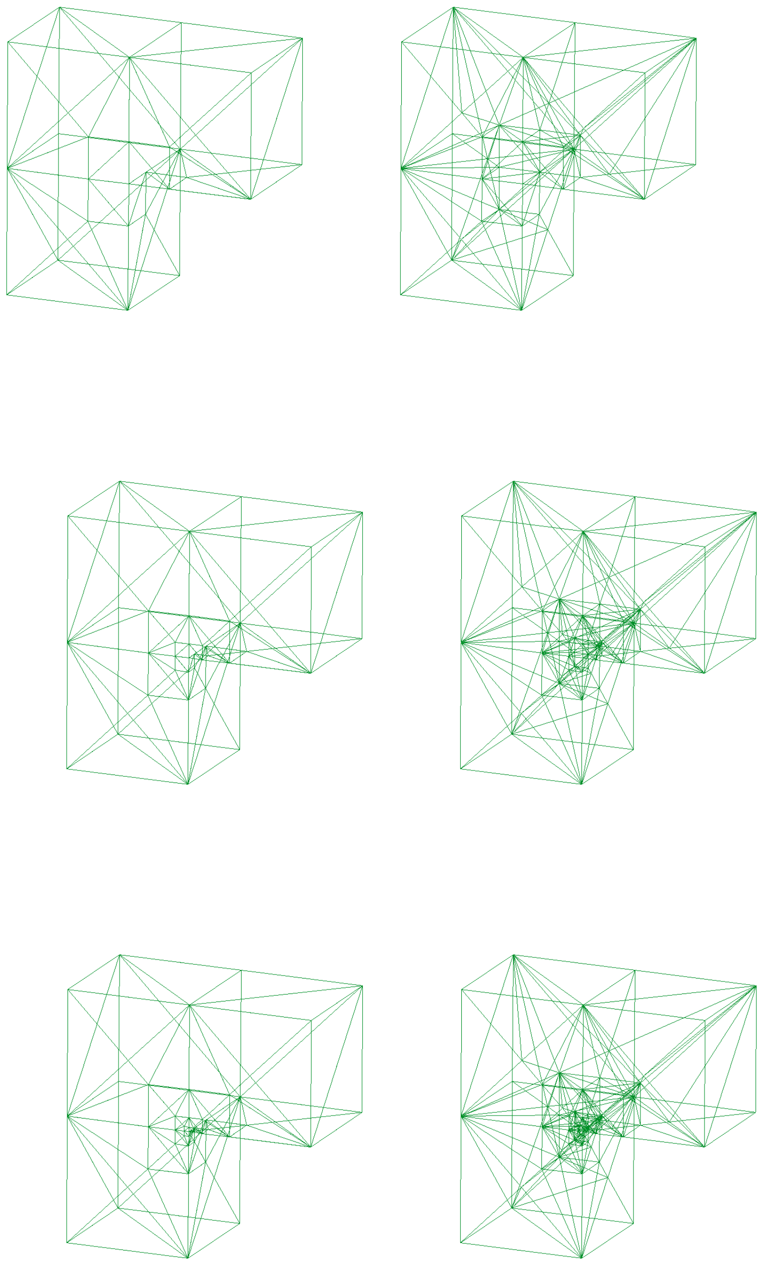

Figure 10. Local mesh refinement of three cubes forming a Fichera-like corner after one, two and three refinement steps. The left figure shows only surface lines.

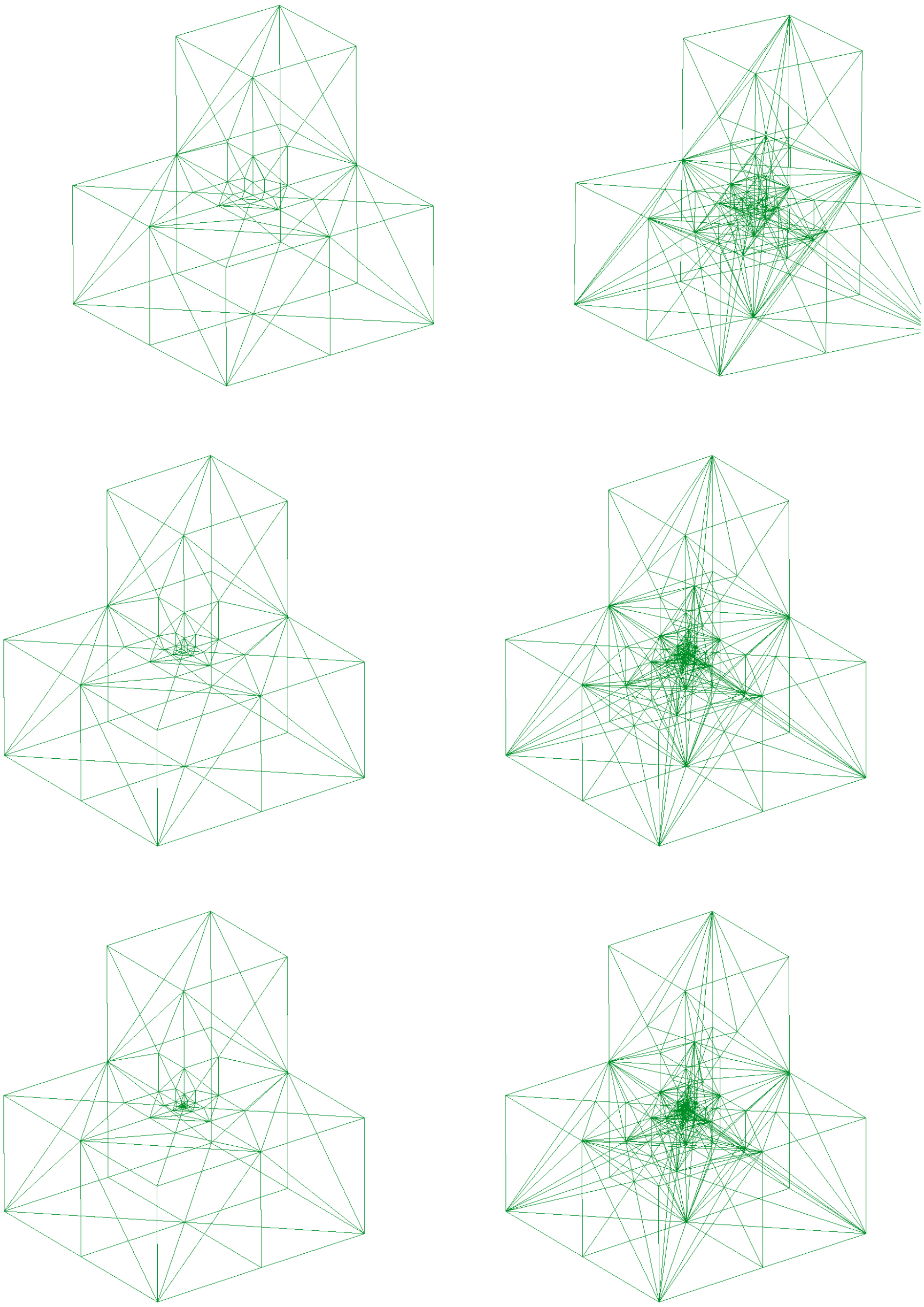

Figure 10. Local mesh refinement of five cubes forming a Fichera-like corner after one, two and three refinement steps. The left figure shows only surface lines.

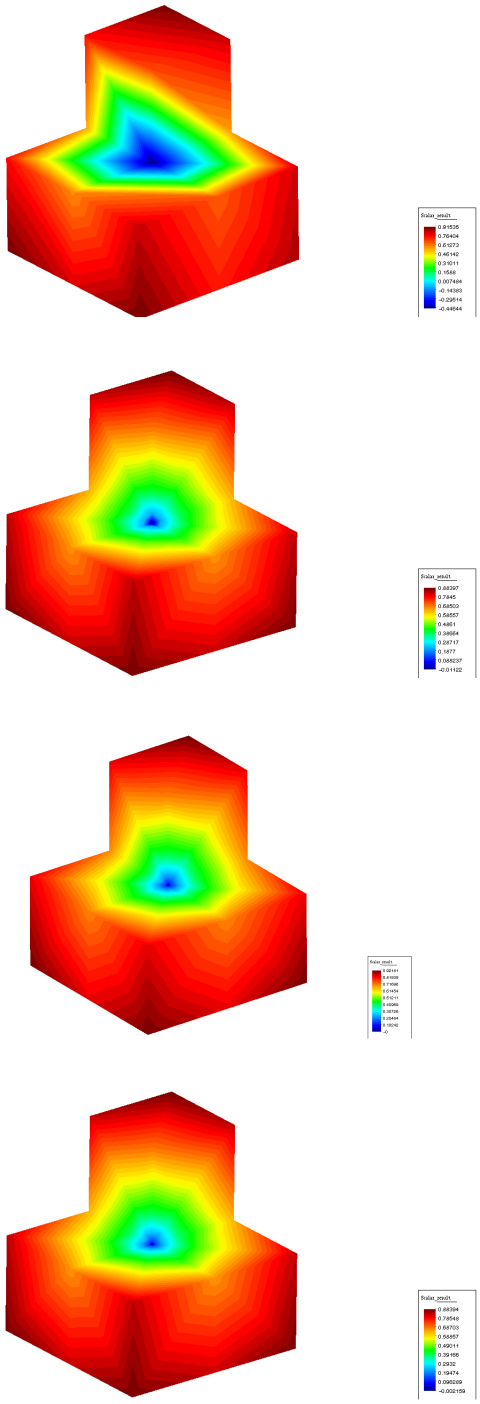

Figure 11. The solution of the Poisson equation for Example 5.2. We present a contour fill of u_h on one, two, three and four times refined mesh.

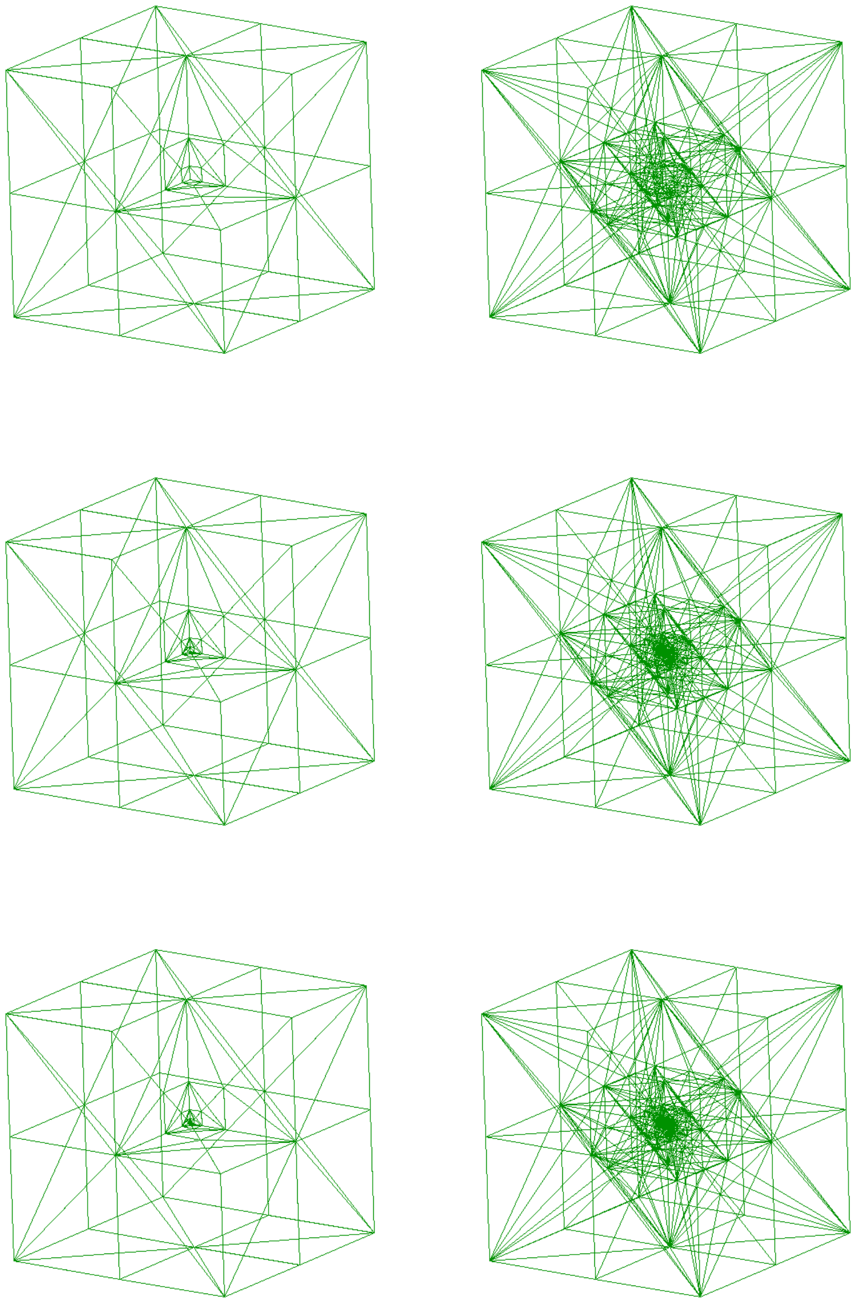

Figure 12. Local mesh refinement of seven cubes forming a Fichera-like corner after one, two and three refinement steps. The left figure shows only the surface lines.

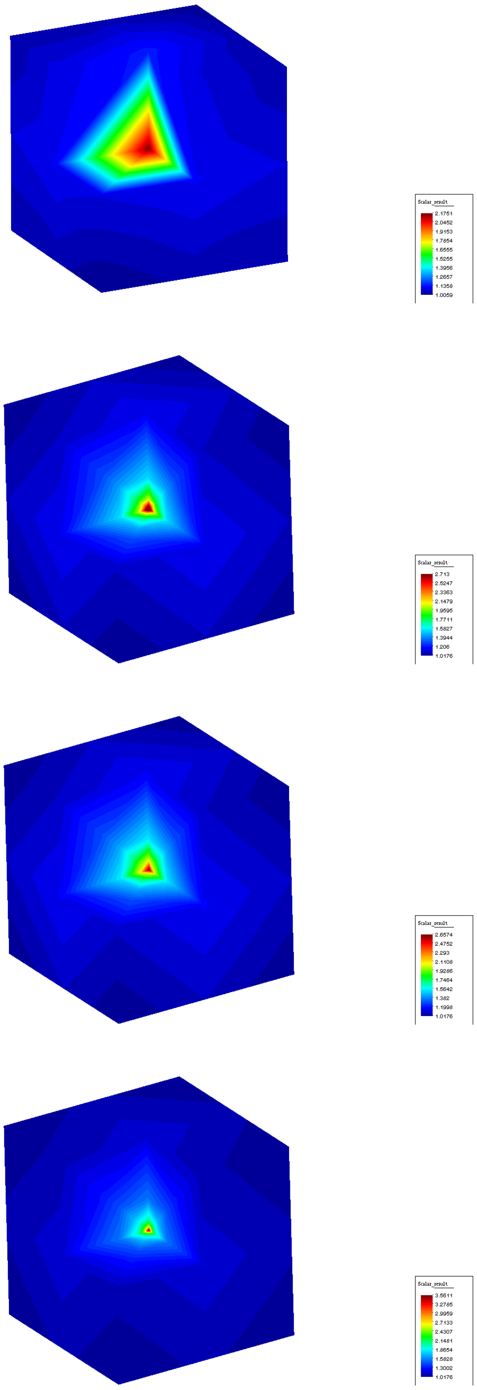

The solution of the Poisson equation for Example 5.3. We present a contour fill of u_h on one, two, three and four times refined mesh.

Acknowledgement. We would like to express our sincere gratitude to Thomas Apel for his valuable comments to this paper.

References

1. T. Apel, *Anisotropic finite elements: Local estimates and applications*, Advances in Numer. Math., B. G. Teubner, Stuttgart, Leipzig, 1999.
2. T. Apel, F. Milde, *Comparison of several mesh refinement strategies near edges*, Comm. Numer. Methods Engrg. **12** (1996), 373–381.
3. T. Apel, S. Nicaise, *The finite element method with anisotropic mesh grading for elliptic problems in domains with corners and edges*, Math. Methods Appl. Sci. **21** (1998), 519–549.
4. M. Bern, P. Chew, D. Eppstein, J. Ruppert, *Dihedral bounds for mesh generation in high dimensions*, Proc. of the Sixth Annual ACM-SIAM Sympos. on Discrete Algorithms (San Francisco, CA, 1995), ACM, New York (1995), 189–196.
5. L. Collatz, *Numerische Behandlung von Differentialgleichungen*, Berlin-Göttingen-Heidelberg, Springer-Verlag, 1951.
6. R. Cools, *Monomial cubature rules since "Stroud": a compilation — part II*, J. Comput. Appl. Math. **112** (1999), 21–27.
7. R. Cools, P. Rabinowitz, *Monomial cubature rules since "Stroud": a compilation*, J. Comput. Appl. Math. **48** (1993), 309–326.
8. M. Dauge, *Elliptic boundary value problems on corner domains*, LN in Math., vol. 1341, Springer-Verlag, Berlin, 1988.
9. M. Feistauer, J. Felcman, M. Rokyta, Z. Vlášek, *Finite-element solution of flow problems with trailing conditions*, J. Comput. Appl. Math. **44** (1992), 131–165.
10. H. Fujii, *Some remarks on finite element analysis of time-dependent field problems*, Theory and Practice in Finite element Structural Analysis, Univ. Tokyo Press, Tokyo (1973), 91–106.
11. S. Korotov, M. Křížek, *Acute type refinements of tetrahedral partitions of polyhedral domains*, SIAM J. Numer. Anal. **39** (2001), 724–733.
12. S. Korotov, M. Křížek, *Local nonobtuse tetrahedral refinements of a cube*, to appear in Appl. Math. Lett. (2003), 1–4.
13. S. Korotov, M. Křížek, P. Neittaanmäki, *Weakened acute type condition for tetrahedral triangulations and the discrete maximum principle*, Math. Comp. **70** (2001), 107–119.
14. M. Křížek, Qun Lin, *On diagonal dominance of stiffness matrices in 3D*, East-West J. Numer. Math. **3** (1995), 59–69.
15. M. Křížek, P. Neittaanmäki, *Finite Element Approximation of Variational Problems and Applications*, Pitman Monographs and Surveys in Pure and Applied Mathematics vol. 50, Longman Scientific & Technical, Harlow; copublished in John Wiley & Sons, New York, 1990.
16. H. Schmitz, K. Volk, W. Wendland, *Three-dimensional singularities of elastic fields near vertices*, Numer. Methods Partial Differential Equations **9** (1993), 323–337.
17. R. S. Varga, *Matrix iterative analysis*, Prentice-Hall, New Jersey, 1962.

Chalmers Finite Element Center Preprints

2001–01 *A simple nonconforming bilinear element for the elasticity problem*
Peter Hansbo and Mats G. Larson

2001–02 *The $\mathcal{LL}^*$ finite element method and multigrid for the magnetostatic problem*
Rickard Bergström, Mats G. Larson, and Klas Samuelsson

2001–03 *The Fokker-Planck operator as an asymptotic limit in anisotropic media*
Mohammad Asadzadeh

2001–04 *A posteriori error estimation of functionals in elliptic problems: experiments*
Mats G. Larson and A. Jonas Niklasson

2001–05 *A note on energy conservation for Hamiltonian systems using continuous time finite elements*
Peter Hansbo

2001–06 *Stationary level set method for modelling sharp interfaces in groundwater flow*
Nahidh Sharif and Nils-Erik Wiberg

2001–07 *Integration methods for the calculation of the magnetostatic field due to coils*
Marzia Fontana

2001–08 *Adaptive finite element computation of 3D magnetostatic problems in potential formulation*
Marzia Fontana

2001–09 *Multi-adaptive galerkin methods for ODEs I: theory & algorithms*
Anders Logg

2001–10 *Multi-adaptive galerkin methods for ODEs II: applications*
Anders Logg

2001–11 *Energy norm a posteriori error estimation for discontinuous Galerkin methods*
Roland Becker, Peter Hansbo, and Mats G. Larson

2001–12 *Analysis of a family of discontinuous Galerkin methods for elliptic problems: the one dimensional case*
Mats G. Larson and A. Jonas Niklasson

2001–13 *Analysis of a nonsymmetric discontinuous Galerkin method for elliptic problems: stability and energy error estimates*
Mats G. Larson and A. Jonas Niklasson

2001–14 *A hybrid method for the wave equation*
Larisa Beilina, Klas Samuelsson and Krister Åhlander

2001–15 *A finite element method for domain decomposition with non-matching grids*
Roland Becker, Peter Hansbo and Rolf Stenberg

2001–16 *Application of stable FEM-FDTD hybrid to scattering problems*
Thomas Rylander and Anders Bondeson

2001–17 *Eddy current computations using adaptive grids and edge elements*
Y. Q. Liu, A. Bondeson, R. Bergström, C. Johnson, M. G. Larson, and K. Samuelsson

2001–18 *Adaptive finite element methods for incompressible fluid flow*
Johan Hoffman and Claes Johnson

2001–19 *Dynamic subgrid modeling for time dependent convection–diffusion–reaction equations with fractal solutions*
Johan Hoffman

2001–20 *Topics in adaptive computational methods for differential equations*
Claes Johnson, Johan Hoffman and Anders Logg

2001–21 *An unfitted finite element method for elliptic interface problems*
Anita Hansbo and Peter Hansbo

2001–22 *A P^2–continuous, P^1–discontinuous finite element method for the Mindlin-Reissner plate model*
Peter Hansbo and Mats G. Larson

2002–01 *Approximation of time derivatives for parabolic equations in Banach space: constant time steps*
Yubin Yan

2002–02 *Approximation of time derivatives for parabolic equations in Banach space: variable time steps*
Yubin Yan

2002–03 *Stability of explicit-implicit hybrid time-stepping schemes for Maxwell's equations*
Thomas Rylander and Anders Bondeson

2002–04 *A computational study of transition to turbulence in shear flow*
Johan Hoffman and Claes Johnson

2002–05 *Adaptive hybrid FEM/FDM methods for inverse scattering problems*
Larisa Beilina

2002–06 *DOLFIN - Dynamic Object oriented Library for FINite element computation*
Johan Hoffman and Anders Logg

2002–07 *Explicit time-stepping for stiff ODEs*
Kenneth Eriksson, Claes Johnson and Anders Logg

2002–08 *Adaptive finite element methods for turbulent flow*
Johan Hoffman

2002–09 *Adaptive multiscale computational modeling of complex incompressible fluid flow*
Johan Hoffman and Claes Johnson

2002–10 *Least-squares finite element methods with applications in electromagnetics*
Rickard Bergström

2002–11 *Discontinuous/continuous least-squares finite element methods for elliptic problems*
Rickard Bergström and Mats G. Larson

2002–12 *Discontinuous least-squares finite element methods for the Div-Curl problem*
Rickard Bergström and Mats G. Larson

2002–13 *Object oriented implementation of a general finite element code*
Rickard Bergström

2002-14 *On adaptive strategies and error control in fracture mechanics*
Per Heintz and Klas Samuelsson

2002-15 *A unified stabilized method for Stokes' and Darcy's equations*
Erik Burman and Peter Hansbo

2002-16 *A finite element method on composite grids based on Nitsche's method*
Anita Hansbo, Peter Hansbo and Mats G. Larson

2002-17 *Edge stabilization for Galerkin approximations of convection–diffusion problems*
Erik Burman and Peter Hansbo

These preprints can be obtained from

`www.phi.chalmers.se/preprints`